RADAR Guide: Standard Methods for Calculating Radiation Doses for Radiopharmaceuticals

Part 1. Collection of Data for Radiopharmaceutical Dosimetry

Michael G. Stabin

Chair, RAdiation Dose Assessment Resource (RADAR) Task Force

Society of Nuclear Medicine and Molecular Imaging

Nashville, TN

Richard E. Wendt III.

Department of Imaging Physics

The University of Texas MD Anderson Cancer Center

Houston, TX

Glenn. D. Flux

Department of Physics, Royal Marsden NHS Foundation Trust,

Sutton, Surrey United Kingdom

Abstract

This paper presents standardized methods for collecting data to be used in performing dose

calculations for radiopharmaceuticals. Various steps in the process are outlined, with some

specific examples given. This document can be used as a template for designing and executing

kinetic studies for calculating radiation dose estimates, from animal or human data.

Introduction

Currently, there is renewed interest in performing radiation dosimetry for radiopharmaceuticals,

particularly in therapy applications. To have any new radiopharmaceutical approved by the US

Food and Drug Administration (FDA), whether for diagnostic or therapeutic applications, human

radiation doses must be estimated. In 1999, Siegel et al. (1) published a guide for obtaining

quantitative data for use in radiopharmaceutical dosimetry. This document, and the companion

document to it (2), updates that information with practical guidance and worked examples.

FDA Requirements for Radiopharmaceutical Dosimetry

The FDA expects pre-clinical studies will be used to determine dosimetry in animals and that

human dosimetry needs to be determined as part of Phase 1, 2, and 3 studies. The Food and Drug

Administration sets standards for the use of lasers (21CFR) and other non-ionizing radiations, food

irradiation, and pharmaceuticals. Medical imaging agents are submitted for approval in:

- Investigational new drug applications (INDs)

- New drug applications (NDAs)

- Biologics license applications (BLAs)

- Abbreviated NDAs (ANDAs)

- Supplements to NDAs or BLAs.

The radiation safety assessment that is associated with the approval of use of medical imaging agents includes many requirements for dose calculations to support these submissions (3):

Applicants should provide a description of which organs have a significant accumulation of activity over time, what activity levels were observed at different times (with at least two time points obtained per phase of radionuclide uptake or clearance), an evaluation of time integrals of activity, descriptions of how they were obtained, and a description of how they were combined with dose conversion factors to obtain doses (if not done by software as noted above). An assessment of significant radiation hazards to other patients and health care workers should also be performed.

USFDA requirements (4) require a 'preclinical phase', in which studies are done in animal species, and Phase 1, 2, and 3 clinical studies, in which dosimetry data are gathered in human subjects, to establish and refine the radiation dose estimates and establish the safety and efficacy of any new drug.

First-in-human' studies can establish the safety and tolerability and preliminary efficacy of a new drug before entering into full-fledged clinical trials...", but all four phases of study are needed to establish the radiation dosimetry of any candidate for a New Drug Application (NDA).

Planning a Study to Obtain Biokinetic Data

In either animal or human studies, one must collect sufficient data to fully characterize the radiation dose (Gy) to all relevant organs and tissues in the body. Siegel et al. (1) note that the key questions in study design are:

'1. What regions are source regions?

2. How fast does the radioactivity accumulate in these source regions?

3. How long does the activity remain in the source regions? How fast is the activity excreted from the source organs?

4. How much activity is in the source regions as a function of time after administration?'

A starting point in considering study design is the physical half-life of the radionuclide employed. Gathering data over several half-lives should give a good evaluation of the complete decay of the compound in the body. A very short-lived nuclide like ^{11}C (which has a 20 min physical half-life) does not afford a long time for gathering image data. Furthermore, one must consider the radiopharmaceutical's *effective* half-time (although usage varies, the term 'half-life' is generally used for physical half-lives, while 'half-time' is generally used for biological and effective half-times.)

$$T_e = \frac{T_b \times T_p}{T_b + T_p}$$

(1)

T_e is the effective half-time, T_p is the radionuclide's physical half-life, and T_b is the compound's biological half-time (the time for half of the activity in a region to be cleared by biological elimination). Physical decay and biological clearance work in parallel to remove radioactivity faster overall than either one would alone. For example, ^{99m}Tc has a 6 hour T_p, so one might think of gathering data over 24-48 hours. However, ^{99m}Tc-DTPA is cleared by the kidneys in just a few short minutes, and from the body overall with about a 1.7 hour biological half-time (5), so 3-10 effective half-times would be 4-13 hours, and many data points would need to be gathered in a relatively short time after administration. A more slowly cleared ^{99m}Tc compound could be

imaged over longer times. A compound labeled with ^{131}I (T_p = 8 days) and whose clearance is relatively slow could possibly be sampled with a few points in the first day, and then one per day for several days. Study design is not an exact science, but care must be taken not to undersample the data when there may be several phases of uptake and clearance. Some radiopharmaceuticals (e.g. ^{131}I tositumomab, tradename Bexxar) are well characterized by a single exponential decay function for the whole body, while others may have two distinct phases of clearance – an early phase that is dominated by rapid clearance of a portion of the administered activity and a later phase that is dominated by slower clearance of the remainder of the administered activity. Of course, physical decay is superimposed upon these biological clearance processes. While it is common for most uptake in organs to be fairly rapid, some organs, tissues and tumors may exhibit an exponential phase of uptake and one or more phases of clearance. In any case, it is important to:

- Capture the early peak uptake and rapid washout phase.

- Cover at least 3-5 effective half-times (T_e) of the radiopharmaceutical. ICRU 67 (6) suggests that points typically be taken near 1/3, 2/3, 1.5, 3, and 5 times the T_e.

- Collect data from at least two time points during the interval in which each biological clearance phase is dominant.

- Account for 100% of the activity at all times.

- Account for all major paths of excretion (urine, feces, exhalation, etc.).

Clinical application of these requirements can be difficult to achieve. For longer lived radionuclides such as ^{131}I and ^{177}Lu, to capture the behavior of early and late clearance phases

may require obtaining multiple data points on the first day, then one point each day for several days afterwards. Obtaining these at times when clinical staff are available and patients can return may present logistical challenges. Siegel et al. (1) analyzed the error that can occur if the uptake and washout phases of clearance are not adequately sampled. For example, Figure D2 of their manuscript (Figure 1) shows the variation of t_{max} (the time for initial sampling) that constrains the error to a given percentage, as a function of effective washout half-time (T_e) for four different values of percentage error ($< 10\%$) in estimates of an organ's Area Under the Curve (AUC) (i.e. the time-integrated activity):

Madsen, et al. demonstrated that when the effective half-time of a mono-exponentially clearing radiopharmaceutical is fairly consistent among patients, the time-integrated activity may be estimated by taking a single measurement at the mean life-time (i.e., 1.443 times the effective half-time) of the radiopharmaceutical. In the case of a bi-exponential clearance, the effective half-time of the longer-lived component should be used. While most of the resulting renal dose estimates in a clinical study of 47 patients who were administered 90Y-DOTATOC were within 10% of those based upon multiple time point imaging, some differed by as much as 22%. They suggest that the population effective half-time may be obtained from a clinical study or from pharmacokinetic modeling. This approach might not be sufficiently accurate, though, when there is a wide variation among patients or even among the source organs within individuals. Stabin (7) provided a more comprehensive analysis of the influence of all parameter values to the overall uncertainty in internal dose estimates.

Extrapolating Animal Data to Humans

In an animal study, the compound under study may be administered to a number of animals which are then sacrificed at different times, with the activity within the organs estimated by

1. counting (harvesting the organs and counting them in a well counter or other device), or perhaps using autoradiography techniques, or

2. imaging of the animals (e.g. with a microPET or microSPECT imaging system). Serial imaging with microimaging systems obviates the need to sacrifice animals, but may complicate the interpretation of the kinetic data that are obtained, as the animals generally need to be anesthetized, which may alter their physiologic state.

The data gathered are then used to predict uptake values in the human from the concentrations seen in the animal tissues (extrapolation). Extrapolation of animal data to humans is by no means an exact science. Crawford and Richmond (8) and Wegst (9) studied some of the strengths and weaknesses of various extrapolation methods that have been proposed in the literature. One method of extrapolating animal data that has been widely applied is the % kg/g method (10) (Kirschner et al. 1975). Using the %/organ or %/g in the animal as the same as the %/organ or %/g in the human is subject to certain pitfalls. In the %-g/kg method, the animal organ data need to be reported as % of injected activity per gram of tissue, and this information plus knowledge of the animal whole body weight are employed in the following extrapolation:

$$\left(\frac{\%}{organ}\right)_{human} = \left[\left(\frac{\%}{g_{organ}}\right)_{animal} x(kg_{TB\ weight})_{animal}\right] x\left(\frac{g_{organ}}{kg_{TB\ weight}}\right)_{human} \qquad (2)$$

The '%' is the percentage of the administered activity, g_{organ} is the mass of the organ in grams, $kg_{TB\ weight}$ is the mass of the whole animal in kilograms. Table 1 shows example calculations of data extrapolated from an animal species to the human using this approach (11):

The animal whole-body weight was 20 g (0.02 kg), and the human source organ chosen had a mass of around 300 g. The human total body weight for the standard adult male of 70 kg was used in the calculations. For example:

$$\frac{38.1\ \%}{g}(animal) \times 0.020\ kg \times \frac{299\ g}{70\ kg} = \frac{3.26\ \%}{organ}(human)$$

Some researchers have also suggested a transformation of the time scale, to account for the differences in metabolic rate among species of different body mass, based on the idea that faster metabolic rates will result in faster clearance of compounds from the body. One suggested scaling approach is given as:

$$t_h = t_a \left[\frac{m_h}{m_a}\right]^{0.25} \qquad (3)$$

where t_a is the time at which a measurement was made in an animal system, t_h is the corresponding time assumed for the human data, and m_a and m_h are the total body masses of the animal species and of the human, respectively. Table 2 shows an example with data extrapolated from an animal species to the human using this time scaling approach (9)

Here the animal whole body weight was 200 g (0.2 kg), and again the human total body weight for the standard adult male of 70 kg was used in the calculations. For example:

$$5 \text{ min} \times \left[\frac{70 \ kg}{0.2 \ kg} \right]^{0.25} = 22 \text{ min}$$

One problem in the area of animal data extrapolation to humans is the treatment of activity that is not accounted for in individual animal organs. Some researchers manage to successfully account for activity in the 'carcass' or rest of the animal body that was not harvested for counting. If the radionuclide is particularly short-lived, this assessment may not be necessary, as one may be able to simply assume that unaccounted for activity was uniformly distributed in other tissues and eliminated only by radioactive decay. For many radiopharmaceuticals this may significantly overestimate the number of disintegrations in these 'remainder' tissues and underestimate the number of disintegrations in excretory organs such as the urinary bladder and the intestines. An assessment of the activity in these regions, via direct counting or analysis of excreta, is usually needed. Such values are usually not extrapolated to humans on a mass basis, but assumed to apply directly (i.e. % excreted by the animal = % excreted by the human); a time extrapolation may be applied if desired. Gathering of excreta data is quite important to accounting for 100% of the administered activity. If it is known that ALL excretion is urinary, one can use (100% minus the

total body retention) as the excreted fraction. If both urinary and intestinal excretion are possible, the collection of both urinary and fecal data is needed.

Sparks and Aydogan (12) investigated the accuracy of animal data extrapolation to humans for a number of radiopharmaceuticals. They reached no solid conclusions that any particular method was superior to another. They did find, however, that extrapolated animal data tend to underestimate human organ self-doses. Figure 2, adapted from Figures 1 and 4 in their publication show two examples of their results. These figures show the ratio of organ 'residence times' (normalized number of disintegrations, which is also proportional to organ self-dose, when no extrapolation (their Figure 1) or both the time and mass extrapolations shown above (their Figure 4) were performed. Values of 1.0 represent perfect agreement, whereas ratios below 1.0 imply that the animal data underpredicted human doses and values above 1.0 imply overestimation of human doses. One would like to see a normal distribution centered around 1.0. The graphs might fit a lognormal distribution, but nonetheless, in most of the cases, extrapolated animal data underpredicted human doses. Thus, providing dosimetry data to the FDA in preclinical studies is necessary in the drug approval process, but in most cases, reasonably accurate human doses will only be derived from the Phase I, II and III clinical studies in human beings.

An important point in the elements of study design that are listed above is to account for 100% of the activity at all times. This is not always easy in preclinical studies, especially for organs that are distributed, such as the musculature and the skeleton, and to the whole body if the carcass of the animal after the removal of specific source organs is too large to be counted unless cut into numerous small pieces. The design of a preclinical study should include how this matter will be addressed, as it might well be too late to obtain this information after the performance of a study that neglects this point.

Steps for Collecting Data in Human Subjects

The external *conjugate view* method, using anterior and posterior projection images from a nuclear medicine camera is the method used most frequently used to obtain quantitative data in human studies for dosimetry. In this method, the source activity A_j is given as(1):

$$A_j = \sqrt{\frac{I_A I_P}{e^{-\mu_e t}}} \frac{f_j}{C} \qquad (4)$$

$$f_j \equiv \frac{(\mu_j \, t_j / 2)}{\sinh \, (\mu_j \, t_j / 2)} \qquad (5)$$

where I_A and I_P are the observed counts over a given time for a given region of interest (ROI) in the anterior and posterior projections (counts/time), t is the average patient thickness over the ROI, μ_e is the effective linear attenuation coefficient for the radionuclide, camera, and collimator, C is the system calibration factor C (counts/time per unit activity), and the factor f represents a correction for the source region attenuation coefficient (μ_j) and source thickness (t_j) (i.e., source self-attenuation correction). Figure 3 shows the geometric relationships. This expression assumes that the views are well collimated (i.e. they are oriented towards each other without offset) and also assumes a narrow beam geometry without significant scattered radiation, septal penetration and other interferences. Corrections for scatter are usually advisable; a number of the proposed methods are described below.

Corrections for Scattered Radiation

One relatively straightforward correction procedure for scatter compensation is the 'Triple Energy Window (TEW) method (13); this involves establishing counting windows on either side of the gamma camera photopeak window such that the area of the two adjacent windows is equal to that of the photopeak (or if not, the count ratios should be appropriately scaled). The corrected photopeak counts (C_T) are given as:

$$C_T = C_{pp} - F_S*(C_{LS} + C_{US}) \qquad (6)$$

where C_{pp} is the total count recorded within the photopeak window, while C_{LS} and C_{US} are the counts within the lower and upper scatter windows, respectively. The scaling factor (F_S) corrects for the (most common) case in which the total width of the scatter windows (in keV) is not equal to that of the photopeak window. It would be unity if they were equal. Thus, adjustment of the adjacent windows is assumed to compensate for the high energy photon scatter tail upon which the true photopeak events ride. Even if the areas of the scatter windows are equal to that of the photopeak window, the use of a scaling factor other than unity may provide the best correction for scatter in a given system with a particular radionuclide. This may be determined by the study of a source of known volume submerged to a realistic depth in a water phantom whose dimensions are similar to that of a human subject (Figure 4). An extension of the triple energy window approach is to use more energy windows and to apply principal component analysis or factor analysis to the resulting data in the energy dimension.

SPECT reconstruction methods have incorporated more sophisticated methods of scatter correction such as estimating the point spread function of the scattering and applying it during the

forward projection of data in an iterative reconstruction algorithm such as maximum likelihood expectation maximization (MLEM).

Commercial SPECT/CT cameras and software have recently been introduced that offer quantitative SPECT in the same manner that PET is quantitative. They include calibrations for specific radionuclides with corrections for attenuation and scatter.

Corrections for Background Activity

When an ROI is drawn over a source region on a projection image, some counts from the region will have originated from activity in the subject's body that is outside of the identified source region. This includes scattered radiation from other ROIs, background radiation, and other sources. Thus a 'background ROI' is drawn over some region of the body that is close to the source ROI and which, in the analyst's opinion, best represents the activity of nearby tissues to the source which will provide the best estimate of a background count rate to be subtracted from the source ROI. As with the scatter correction shown above, a scaling factor may be needed to correct the number of counts in the background ROI so that the appropriate correction is made, given the number of pixels in the source and background ROI. Alternately, one may simply subtract the number of counts per pixel in the background ROI from the number of counts per pixel in the source ROI and then calculate the total number of counts in the source ROI as the corrected number of counts per pixel times the number of pixels.

A quality assurance check is to place a source of activity of the radionuclide being imaged external to the body. Then an ROI is drawn away from the subject's body, and also away from any "star pattern" streaks that may accompany the source image due to septal penetration, but close enough

that it captures a typical number of counts per pixel that represents background and scattered radiation within the imaging area close to the subject. The counts of this source over time should reflect the radionuclide physical half-life

It is important to avoid drawing a background ROI over body structures that may contain a high level of activity (e.g. blood vessels and areas of the skeleton with significant uptake), as this will remove too many counts from the source ROI. It is also important to not draw the background ROI too far away from the source region in an area of particularly low background, as this may not remove enough counts from the source ROI. The choosing of locations and sizes of background ROIs is very difficult to prescribe exactly, and practices vary considerably among investigators, which can result in markedly different results for the final estimates of activity assigned to a source ROI. This process should be carried out with care and attention to the above points for the best and most reproducible results. The locations of the background ROIs should be documented, perhaps by graphical screen captures if necessary, to enhance the reproducibility of a dosimetric analysis.

Pereira et al. (14) showed examples of optimized background regions for regions in a water phantom representing organs of interest (Figure 5), noting possible uncertainties in different quantification methods.

Correction for Overlapping Organs and Regions

It is not uncommon for some organs or tumors to overlap other structures in projection images. The right kidney and the liver are frequently partially superimposed in such images, as are the left kidney and spleen, in many subjects. When organ overlap occurs, an estimate of the total activity

within a source can be obtained by various approximate methods. For paired organs, such as the kidneys and lungs, one approach is simply to quantify the activity in one of the organs for which there is no overlap with other organs and double the number of counts in this organ to obtain the total counts in both organs. If the masses of the paired organs can be determined, perhaps using volumes that are derived from CT or MR image and are then multiplied by the tissue density, then the scaling factor could be the combined masses of the two organs divided by the mass of the organ without overlap. Another approach is to draw an ROI over the region of the organ that has no overlap in scans where there is overlap, count the number of pixels, note the average count rate per pixel, then use an ROI from another image in which there is no apparent overlap and the whole organ is clearly visible, count the number of pixels in a larger ROI drawn on this image, and then simply multiply the count rate per pixel from the first image by the number of pixels in the second image in order to estimate the total counts from the organ in the first image. Or, equivalently, take the total number of counts in the partial organ ROI in the first image and multiply by the ratio of the numbers of pixels in the ROIs in the second and the first images respectively. If no image can be found in which a significant overlap with another organ does not obscure the organ boundaries, an approximate ROI may need to be drawn just from knowledge of the typical shapes of such organs. This kind of approximation is obviously not ideal, but it may be necessary.

Obtaining Gamma Camera System Attenuation and Calibration Coefficients

Attenuation Coefficient. The system attenuation coefficients (μ_e), both for the nuclide to be imaged, and the nuclide used to establish the body thickness for the attenuation correction (typically ^{57}Co) , must be measured at some time before (or possibly after) radiopharmaceutical administration in a separate experiment. The procedure involves preparation and counting of a

source of activity, ideally one whose surface area is greater than that of the source region with the same radionuclide and the same gamma camera settings as those that are to be used for the patient imaging study. As an example, for small regions one may fill the bottom of a Petri dish (covered and sealed to prevent possible contamination); for large regions, fill a flood source. A small, point-like source can also be used, if necessary. The source should be counted for a fixed time (e.g. 5 minutes) in air, with no intervening attenuating material. Then, the measurement is repeated with several different thicknesses of attenuating material of approximately unit density (i.e. 1 g/cc) between the source and one of the gamma camera heads. One may obtain the count rates by drawing ROIs encompassing the source region (with correction for background in an adjacent ROI) and then plot the background-corrected counts in the ROIs vs. the interposed attenuator thickness (another method for acquiring transmission data is to acquire a transmission scan of the stacks of attenuating material using a line or flood source). The counts may be fit by an exponential function, or the natural logarithm of the counts may be fit by a straight line. In either case, the factor μ_e that best fits the data is the attenuation coefficient to be used in corrections in patient studies.

System calibration factor. As with the attenuation coefficient, the system calibration factor, C, must be measured at some time before or after radiopharmaceutical administration in a separate experiment. For this factor, the method is to prepare a standard of known activity of the same radionuclide as that to be used for administration to subjects, usually a few tens of MBq in almost any suitable container (e.g. a syringe or vial). The exact source strength is not important, as long as sufficient counts are obtained for a consistent evaluation over the course of the study, and as long as not too many counts are obtained, resulting in count saturation and possibly

dead time in the camera. The standard should be counted in air for a fixed time (e.g. 5 minutes) at a source-to-collimator distance which approximates that of the patient midline distance used for the imaging study (Figure 6)

The count rate per unit activity (in units of, e.g., cpm/Bq) represents the calibration factor. The collimator count-rate response as a function of the source-to-collimator distance must be known. For parallel-hole collimators, the collimator efficiency is invariant near the center of the field of view; however, for other collimators, such as diverging, converging, and pinhole collimators, the efficiency is dependent upon the source-to-collimator distance. It is also important to employ the same camera settings, such as the width of the energy window, for this calibration as for the patient imaging.

In most cases the self-attenuation factor f is not significantly different from unity and is rarely important. Normally, one assumes that the variation in body thickness across individual ROIs is small, and so a single attenuation factor may be used to calculate the activity for the entire ROI. On the other hand, if the ROI is large and body thickness is thought to vary substantially within the ROI, a pixel-by-pixel calculation may be made. A pixel-by-pixel attenuation calculation can always be made, regardless of this assumption. A conjugate-view measurement is thus made at each of the time points chosen and the best ROIs for each region are superimposed on the images at each time. Because of potentially different rates of uptake and clearance in various tissues, individual organs or tumors may be best visualized at different times after administration. Some regions have most of their uptake early and clear quickly, while others may accumulate activity more slowly. Thus, different times may be chosen at which to draw the best ROIs for different regions. The best approach is to have a computer program that allows the ROIs to be

independently defined and saved, but then linked together and moved together, to allow the

relative locations of all ROIs to be retained when new ROIs are defined, or when different

patient images reflect slightly different patient placement on the imaging table or slightly

different patient orientation towards the camera heads. Care should be taken to have the patient

recline in the same position in all images, as differences in patient orientation towards the camera

heads may change the lateral separation between organs. One aid in achieving this are the

cushions that are used to stabilize the patient and produce reproducible positioning in radiation

oncology.

Use of Tomographic Data in Quantitative Imaging

The use of tomographic data, either Single Photon Emission Computed Tomography (SPECT) or

Positron Emission Tomography (PET), for quantitative image analysis for dosimetry overcomes

some of the problems inherent in anterior-posterior planar imaging. The advent of hybrid

SPECT/CT cameras enables improved attenuation correction while iterative reconstructions

techniques allow correction for scattering and for depth-dependent resolution. The first

quantitative SPECT/CT systems for implementing voxel-based dosimetry are appearing

commercially. Scatter and attenuation corrections are inherently applied in the image

reconstruction process. An important problem in planar imaging is organ overlap. For example,

the right kidney is usually partially or totally obscured by the liver. Tumors may also be difficult

to delineate because of other overlying structures with significant activity. In the case of PET,

routine calibrations for clinical diagnoses ensure that the data provided are already quantitative

and can be used directly for dose calculations. In SPECT, clinical needs normally do not

necessitate an absolute activity quantification. Performing quantitative SPECT for internal dose calculations is somewhat more difficult than planar imaging, but for the reasons noted above, may offer desirable advantages. Dewaraja et al. (15) provided an overview of methods to perform quantitative SPECT for radionuclide therapy. The steps that they outlined were:

1. Acquisition

2. Dead time corrections

3. Image reconstruction

4. Compensation for image-degrading effects: attenuation, scatter, and detector response

5. Definition of targets

6. Determining the camera calibration factor

7. Performing partial volume corrections

8. Integrating the time-activity curves

As SPECT image acquisition and quantification is more difficult and time consuming than planar imaging, and each CT scan for attenuation imparts an additional radiation absorbed dose to the patient, one may employ a 'hybrid' method – using a series of planar images to establish the overall biokinetic behavior, with one or more SPECT images taken concurrently with a planar image, to better establish absolute accuracies (Figure 7).

At the time that this is being written, new technology both in PET and in SPECT is promising to improve the accuracy of dosimetric workups by enabling volumetric imaging. Two recently introduced commercial long axial extent PET systems might be characterized as "whole body." One has a two-meter axial field of view, which can literally image the entire body of most patients at once. The other has a 106 cm axial field of view, which is designed to be able to image most patients from the crown of the head to mid-thigh. These systems have much higher

sensitivity compared to more typical PET scanners and thus can acquire useful data over a longer portion of the time-activity curve, which should improve the estimation of the time-integrated activity. They also acquire the entire volume simultaneously, which again improves the time-activity curve.

Whole body SPECT is available in preclinical instrumentation. That technology is reportedly being scaled up to accommodate adult human beings. Novel SPECT technology that was originally developed for cardiac imaging acquires data from many points of view in such rapid succession that it is effectively simultaneous in three dimensions over the time-scale of the physiological processes of interest in internal dosimetry. That technology has been built into a full-ring SPECT camera with an axial field of view of roughly 60 cm. Although its cadmium-zinc-telluride (CZT) detectors are better suited to low and medium energy radionuclides than to high energy radionuclides, its higher sensitivity and better energy resolution allow SPECT scans of many radionuclides to be acquired in the time that an ordinary gamma camera requires for a planar whole-body scan.

Figure 1. Reprinted from Figure D2 by Siegel et al. (*1*), showing the variation in tmax to constrain the error on Area Under the Curve (AUC) to a fixed percent.
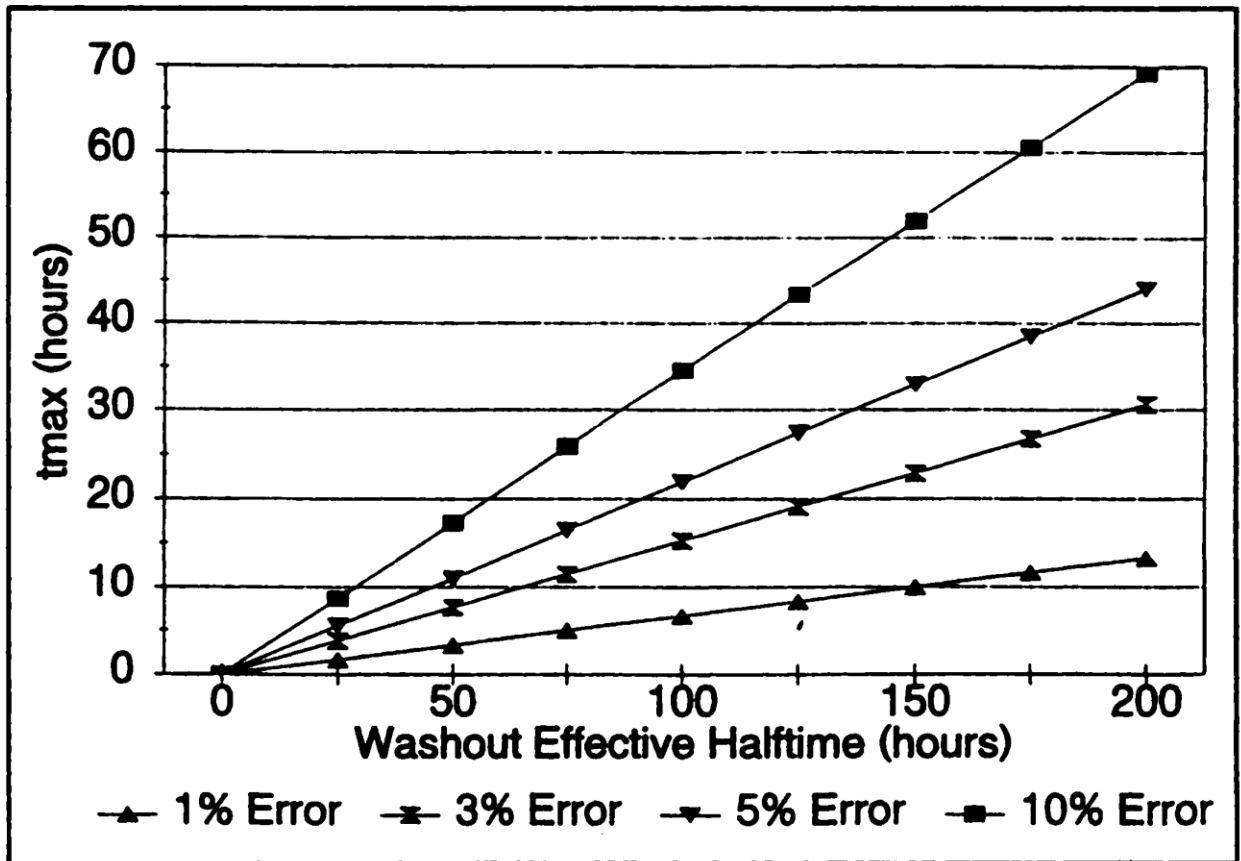
Figure 2: Adaptation of figures from Sparks and Aydogan (*12*), showing the frequency distribution of the ratio of organ residence times using raw data or time and mass extrapolated data from animals to humans
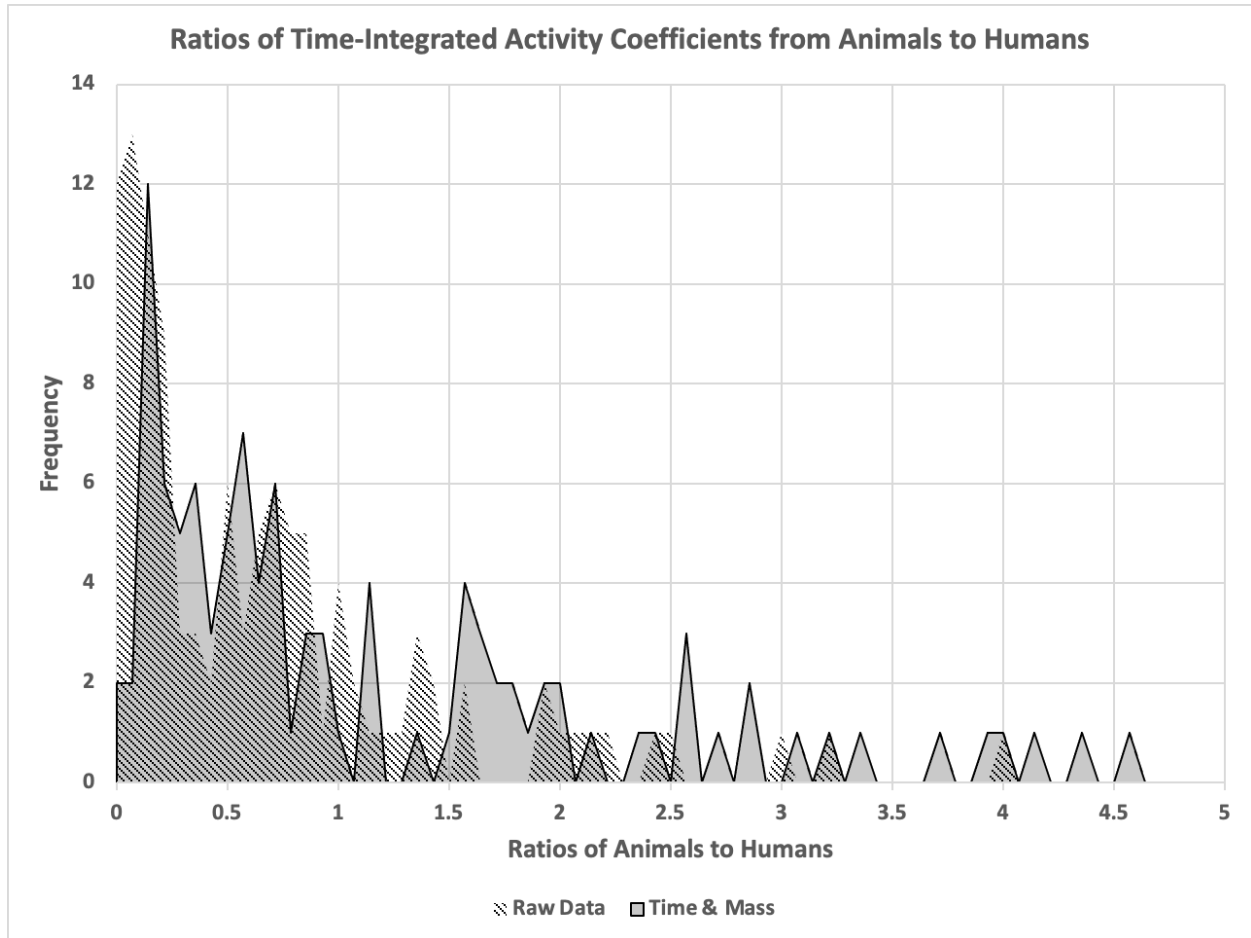

Ratios of Time-Integrated Activity Coefficients from Animals to Humans

Figure 3. Geometric representation of the correction for attenuation in the Geometric Mean method. t is the total thickness of the subject while t1 is the depth of the middle of the source from the upper surface and t2 is the depth of the source from the lower surface. t=t1+t2. The product of the upper and lower attenuation factors is dependent only upon the total thickness and not the position of the source within the subject.
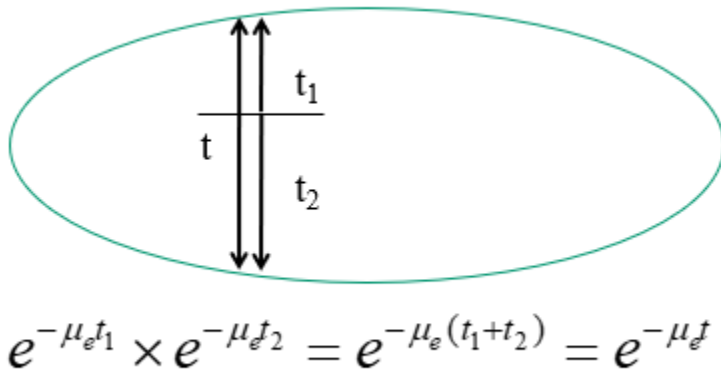
$$e^{-\mu_e t_1} \times e^{-\mu_e t_2} = e^{-\mu_e (t_1+t_2)} = e^{-\mu_e t}$$

Figure 4. Example of the use of multiple windows to correct for scattered radiation in gamma camera images. The ideal spectrum of Ho-166 is plotted in blue and the spectrum blurred by the energy resolution of a gamma camera is plotted in orange. The upper scatter window captures down-scatter from the high energy gamma rays while the lower scatter window captures the down-scatter from the 81 keV gamma ray as well. The weighting factor of 0.65 on the lower scatter window was determined empirically.
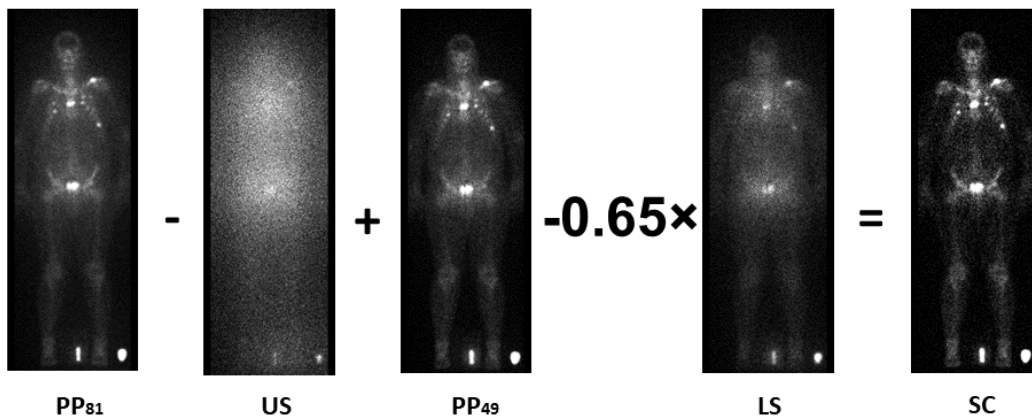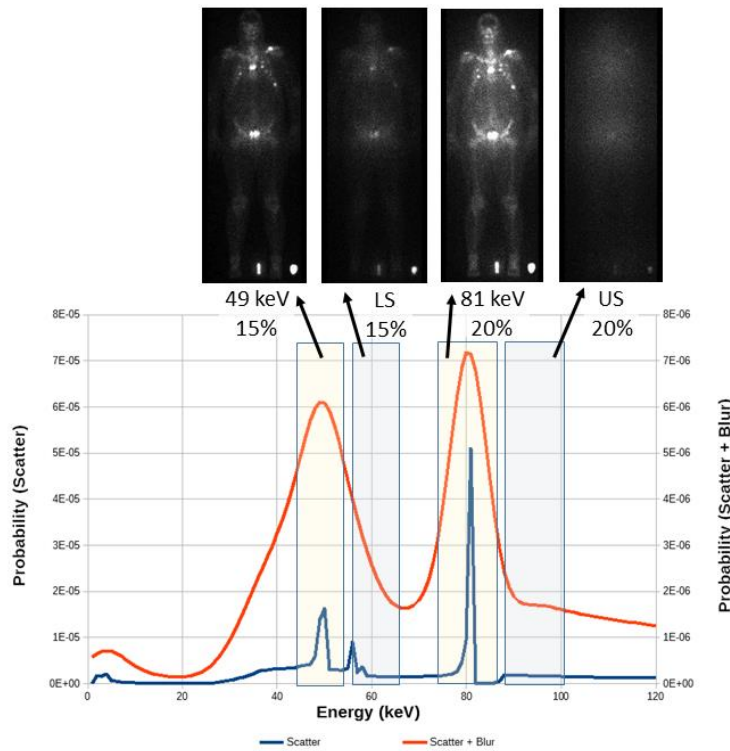
Figure 5. Background regions drawn by Pereira et al. in a water phantom. The background region is positioned over an area near the source that has the count density of the object in the absence of the source. Reprinted from (*14*).
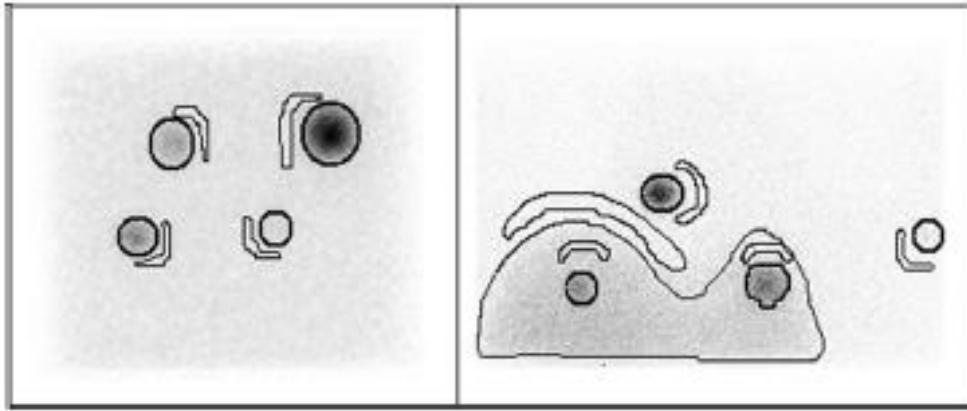
Figure 6. Use of point source to establish system calibration coefficient.

Effective Point Source

$$A(\mu Ci) = \frac{N_{Detector[cps]}}{Sensitivity_{[cps/\mu Ci]}}$$
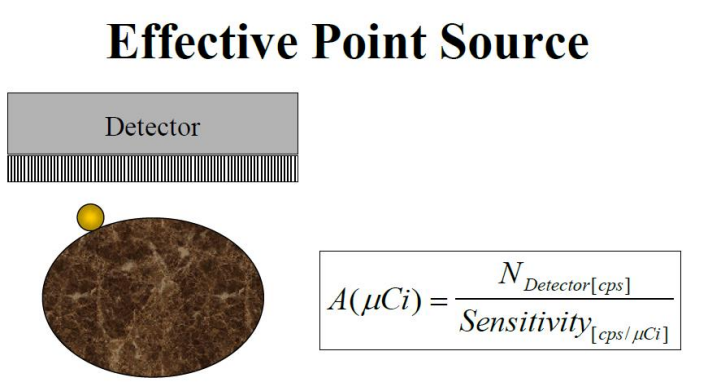
Figure 7. Combining SPECT and Planar images for activity quantification. Planar images are acquired at every time point while quantitative SPECT/CT images are acquired only at one time point. A volume of interest containing a source in the SPECT images is then used to calibrate the counts from the same source in the planar images.
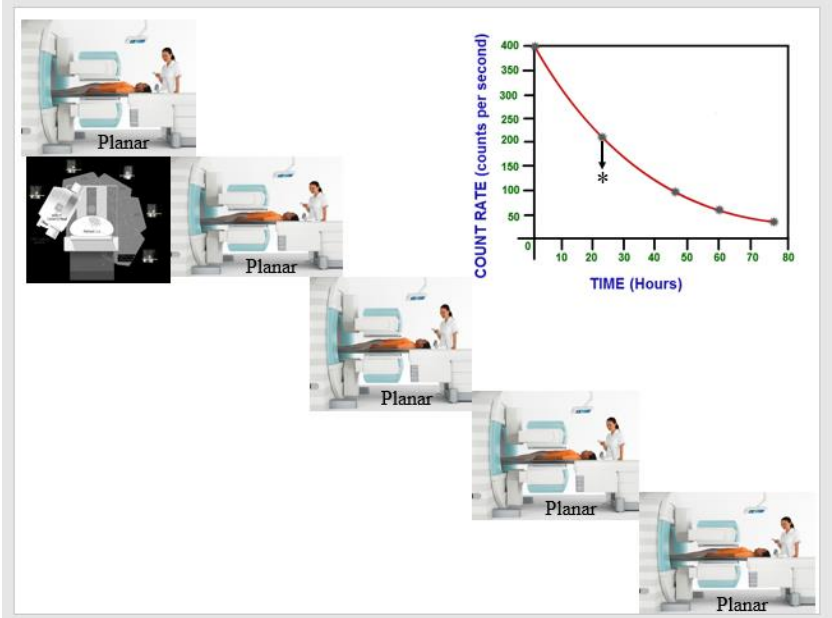
Table 1. Animal Data Extrapolation Example (Mass Extrapolation).

	Source Organ				
ANIMAL	**1 hr**	**3 hr**	**6 hr**	**16 hr**	**24 hr**
%ID/organ	3.79	3.55	2.82	1.02	0.585
(%ID/g)	38.1	36.6	30.8	11.3	5.70
HUMAN					
%ID/organ	3.26	3.12	2.63	0.962	0.486

Table 2. Animal Data Extrapolation Example (Time Extrapolation).

Animal Time Scale	5 min	15 min	30 min	60 min	1.5 h
Extrapolated Human Time Scale	22 min	1.1 h	2.2 h	4.3 h	6.5 h

References

[1] Siegel J, Thomas S, Stubbs J et al. MIRD Pamphlet No 16 – Techniques for Quantitative Radiopharmaceutical Biodistribution Data Acquisition and Analysis for Use in Human Radiation Dose Estimates. J Nucl Med 40:37S-61S, 1999.

[2] Stabin MG, Wendt III, RE, Flux, GD. RADAR Guide: Standard Methods for Calculating Radiation Doses for Radiopharmaceuticals. Part 1. Collection of Data for Radiopharmaceutical Dosimetry. J Nucl Med, in press.

[3] US Food and Drug Administration. Guidance for Industry Developing Medical Imaging Drug and Biological Products, Part 1: Conducting Safety Assessments. June 2004.

[4] https://www.fda.gov/ForPatients/Approvals/Drugs/ucm405622.htm

[5] International Commission on Radiological Protection. Radiation Dose to Patients from Radiopharmaceuticals. ICRP Publication 53, Pergamon Press, New York, 1988.

[6] International Commission on Radiological Units and Measurements. Absorbed-Dose Specification in Nuclear Medicine. International Commission on Radiation Units & Measurements, Inc. Bethesda, MD, 2020.

[7] Stabin MG. Uncertainties in Internal Dose Calculations for Radiopharmaceuticals. J Nucl Med 2008; 49:853–860.

[8] Crawford DJ, Richmond CR. Epistemological considerations in the extrapolation of metabolic data from non-humans to humans. In Third International Radiopharmaceutical Dosimetry Symposium, E Watson, A. Schlafke-Stelson, J Coffey and R. Cloutier eds. US Dept of Health, Education, and Welfare, 1981, pages 191-197.

[9] Wegst A. Collection and presentation of animal data relating to internally distributed radionuclides. In Third International Radiopharmaceutical Dosimetry Symposium, E Watson, A. Schlafke-Stelson, J Coffey and R. Cloutier eds. US Dept of Health, Education, and Welfare, 1981, pages 198-203.

[10] Kirschner A, Ice R, Beierwaltes W. Radiation dosimetry of ^{131}I-19-iodocholesterol: the pitfalls of using tissue concentration data, the author's reply. J Nucl Med 16(3):248-249, 1975.

[11] Stabin MG. Fundamentals of Nuclear Medicine Dosimetry. Springer, New York, NY, February 2008.

[12] Sparks R, Aydogan B. Comparison of the effectiveness of some common animal data scaling techniques in estimating human radiation dose. In: Proc. Sixth International Radiopharmaceutical Dosimetry Symposium, Oak Ridge Institute for Science and Education, 1999, pp 705-716.

[13] Ogawa K, Harata Y, Ichihara T et al. A practical method for position-dependent Compton-scatter correction in single emission CT. IEEE Trans Med mag , 1991, 408-412.

[14] Pereira JM, Stabin MG, Lima FRA et al.. Image Quantification For Radiation Dose Calculations—Limitations And Uncertainties. Health Phys. 99(5):688 –701; 2010.

[15] Dewaraja YK, Frey EC, Sgouros G et al. MIRD Pamphlet No. 23: Quantitative SPECT for Patient-Specific 3-Dimensional Dosimetry in Internal Radionuclide Therapy. J Nucl Med 2012; 53:1310–1325.